IEEE Access
Multidisciplinary | Rapid Review | Open Access Journal

Received August 10, 2019, accepted November 7, 2019, date of publication November 12, 2019, date of current version November 27, 2019.

Digital Object Identifier 10.1109/ACCESS.2019.2953204

Study on the Influence of Plane Coil Geometric Parameters on Initial Launch Velocity

ENLING TANG, TIANZHI ZHENG, YAFEI HAN, AND CHUANG CHEN
Intensive Dynamic Load Research Center, Shenyang Ligong University, Shenyang 110159, China

Corresponding author: Enling Tang (tangenling@126. com)

This work was supported in part by the National Natural Science Foundation of China under Grant 11472178, in part by the Open Foundation of Hypervelocity Impact Research Center of the Cardc-China Aerodynamic Research and Development Center (CARDC) under Grant 20181201, and in part by the Open Project of State Key Laboratory of Explosion Science and technology in Beijing Institute of Technology under Grant KFJJ18-04M, to provide fund for conducting experiments.

ABSTRACT Active electromagnetic armor, as a kind of electromagnetic launch, is a future-oriented high-tech weaponry. The geometric parameters of the coil are the key elements affecting the interception performance. In this paper, the influence of copper strip length, copper strip thickness and radius of the base circle on the initial launch velocity of the intercepting plate was studied based on the self-developed launcher. The relationship between the length of the copper strip and the initial velocity was theoretically deduced. The reliability of the simulation was verified by a combination of simulation and experiment. The results show that the initial velocity of the intercepting plate is linear with the winding length of the coil. As the width of the copper strip increases, the initial velocity increases accordingly, and the radius of the base circle has little effect on the initial velocity of intercepting plate.

INDEX TERMS EML (electromagnetic launch), coil geometric parameters, intercepting plate, electromagnetic coupling, initial launch velocity.

I. INTRODUCTION

Electromagnetic launch technology is a new concept technology based on pulse power and pulsed intense magnetic field technology [1], [2]. It relies on the interaction between the electromagnetic field generated by the pulsed power source and the mutual current generated in the metal plate, so that the metal plate is launched by a electromagnetic force. Electromagnetic launch technology is widely used in the military [3]. Electromagnetic launch technology has been successfully applied to the electromagnetic guns and the launch of the spacecraft [4], and the active electromagnetic protection of armored vehicles [5]–[7], and electromagnetic interception defense of ships and fixed-point targets [2] are also underway. Chinese scholars have done a lot of work on the launch principle, electromechanical characteristics and even performance optimization of active electromagnetic armor. Jin Hong-Bo [7] applied uniform design and numerical simulation technology to optimize the structure of the coil. Yuan Chi [8] focused on the problem of eddy current distribution in the EML armor plate. Wang Yezhong and Xu Hui [9], [10] established system state equation based on the principle of virtual displacement, calculated the mutual inductance change law during the launching process and applied the numerical simulation to study the influence of mechanical structure on launching ability. In this paper, the influence of the base circle radius, the thickness of the copper strip and the length of the copper strip on the initial velocity of the launching plate is studied based on the following 3 considerations.

1)For a long time, for the convenience of inductance calculation, the coil is often simplified into a number of coaxial equidistant rings [7]–[10]. Although this can simplify the calculation and keep the calculation accurate, it is quite different from the actual condition. The main reason is that the coil is difficult to form an integer circle.

2) When studying the influence of the geometric parameters of the coil on the initial velocity of the flying plate, focusing on the independent parameters such as the number of turns and the spacing of the turns will make the generality of the obtained law poor, and thus the variable will be too much.

3) From the point of view of the processing of the coil, it is not easy to control the spacing of the turns, but easy to

The associate editor coordinating the review of this manuscript and approving it for publication was Chong Leong Gan.

TABLE 1. Basic parameters of the coil.

Copper strip length/L (mm)	Copper strip thickness/S (mm)	Coil base radius/r (mm)	Coil outer radius/R(mm)	Nominal turns/n	Nominal spacing/P (mm)	Coil code
2000	2	15	76	6.999	8.715	C1
2500	2	15	76	8.749	6.972	C2
3000	2	15	76	10.499	5.810	C3
3500	2	15	76	12.249	4.980	C4
4000	2	15	76	13.999	4.358	C5
4500	2	15	76	15.749	3.873	C6
5000	2	15	76	17.498	3.486	C7
5500	2	15	76	19.248	3.169	C8

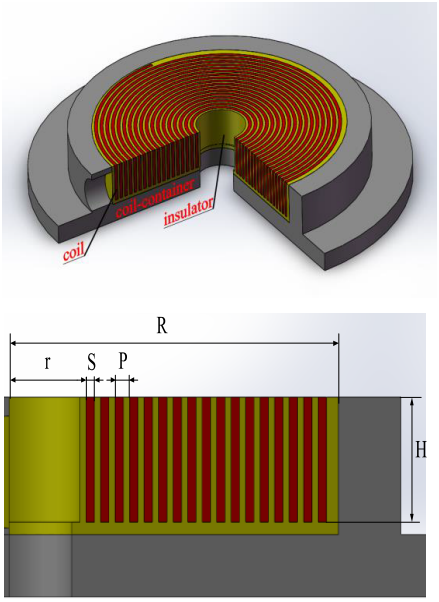

FIGURE 1. Model of coil system.

control the parameters and winding parameters of the copper strip. Based on the copper strip parameters and winding parameters, relevant research is carried out, which is highly compatible with the actual processing conditions.

Therefore, based on the past research, this paper attempts to concentrate on the geometric parameters and winding parameters of the copper strip, and reveals its influence on the launch performance.

II. STRUCTRAL PARAMETERS OF THE COIL

Figure 1 shows the launch system model. If a copper strip with a certain length, thickness, and height is wound by a mandrel with a certain radius and placed in a coil-container with a certain inner radius, after the coil rebounds, the coil is approximately radially evenly distributed and its geometry can be determined by the following relationship:

$$N = L/\pi(r + R) \tag{1}$$

$$P = \pi(R^2 - r^2)/L \tag{2}$$

where N is the nominal number of turns of the coil, which can be a decimal; P is the nominal adjacency spacing. Table 1 shows the basic parameters of the coil.

In Table 1, the meaning of decimal turns is that the strip is not wound into an integer circle. When the calculated value of the spacing is smaller than the thickness, the adjacent two copper strips partially overlap, and the model of this case should be discarded. In fact, when P-S <1.5mm, It is already difficult to inject epoxy resin forming insulator. Therefore, although the case of P-S ≈1mm has been studied, its meaning is only for reference.

III. THEORETICAL DERIVATION

According to the basic principles of electromagnetics, the inductance energy of the system at any moment is:

$$Wl = \frac{1}{2}Li^2 \tag{3}$$

where L is the inductance of the whole sysytem, and i is the current. According to the principle of virtual displacement:

$$F = -\frac{dWl}{dx} \tag{4}$$

x is the displacement of the flying plate. F is the force acting on the flying plate. If the inductance change caused by the coil deformation during the launching process is neglected, the change of the inductance only includes the change of the mutual inductance between the coil and the flying plate caused by the displacement. Therefore:

$$F = -\frac{dWl}{dx} = -\frac{dM(x)}{dx}i^2 \tag{5}$$

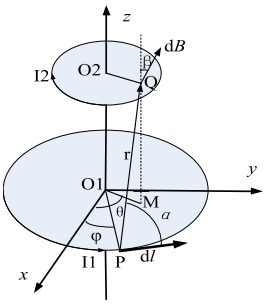

FIGURE 2. Schematic diagram of mutual inductance calculation of coaxial loop.

$$a = F/m \tag{6}$$

$$v = \int adt \tag{7}$$

Relationship between mutual inductance and displacement during launch can be expressed[9]:

$$M(x) = M_0 e^{-qx} \tag{8}$$

In the above formula, M_0 is the mutual inductance in the initial position of the flying plate. Combining the current equation of the RLC circuit [11] and assuming that the plate does not have significant displacement during acceleration, it can be derived from (5) to (8) as [10]:

$$vm = \frac{M_0 q e^{-qx_0} U_0^2 C}{2mR} \tag{9}$$

where U_0 is the initial charging voltage of the capacitor; C is its capacitance; R is the total resistance of the loop, and x_0 is the distance between the flying plate and the coil at initial position. It can be seen from (9) that the initial launch velocity is proportional to the mutual inductance gradient in initial position; inversely proportional to the loop resistance. The resistance of copper strip with 6 meters long, 2 millimeters thick and 20 millimeters wide is 2.6 $m\Omega$, which far less than the one of the loop-30 $m\Omega$. At high frequencies, the loop resistance and the strip resistance increase accordingly. Therefore, when changing the length of the copper strip, the total resistance of the loop does not change significantly. The following is the theoretical derivation and calculation about the relationship between the length of the copper strip and the inductance gradient in initial position.

Let $P(R_1 cos\varphi,\ R_1 sin\varphi,0)$, $Q(x,\ y,\ d)$, $M(x, y, 0)$, and $\overrightarrow{r}$ $(x\text{-}\ R_1 cos\varphi,\ y\text{-}\ R_1 sin\varphi,\ d)$, $\overrightarrow{O1P}(\mathrm{R_1 cos\varphi},\ \mathrm{R_1 sin\varphi},\ 0)$, $d\overrightarrow{l}$ $(-\tan\varphi,1,0)$. According to Biot-Safar's law, the magnetic flux density at point Q is

$$d\overrightarrow{B} = \frac{\mu_0}{4\pi} \frac{Id\overrightarrow{l} \times \overrightarrow{r}}{r^3} \tag{10}$$

Its direction vector is:

$$\left(\frac{d\cos\varphi}{x\cos\varphi + y\sin\varphi - R_1}, \frac{d\sin\varphi}{x\cos\varphi + y\sin\varphi - R_1}, -1\right)$$

β is the angle between $d\overrightarrow{B}$ and axis z, and

$$\cos\beta = \frac{x\cos\varphi + y\sin\varphi - R_1}{\sqrt{d^2 + (x\cos\varphi + y\sin\varphi - R_1)^2}}; \alpha$$

is the angle between $d\overrightarrow{l}$ and $\overrightarrow{r}$, and

$$\sin\alpha = \sqrt{\frac{(x\cos\varphi + y\sin\varphi - R_1)^2 + d^2}{(x - R_1\cos\varphi)^2 + (y - R_1\sin\varphi)^2 + d^2}}.$$

The component of the magnetic flux density along axis z: $dB_z = \frac{\mu_0}{4\pi} \frac{I_1 d\overrightarrow{l}\ \sin\alpha\cos\beta}{r^2}$

Let $dl = R_1 d\varphi$, so: $dB_z = \frac{\mu_0 R_1 I_1}{4\pi r^2} \sin\alpha\cos\beta d\varphi$

$$= \frac{\mu_0 R_1 I_1}{4\pi} \frac{x\cos\varphi + y\sin\varphi}{[(x - R_1\cos\varphi)^2 + (y - R_1\sin\varphi)^2 + d^2]^{3/2}} d\varphi$$

Then the Z-direction magnetic flux density from the *Coil1* at the Q is B_z

$$B_z = \frac{\mu_0 R_1 I_1}{4\pi} \int_0^{2\pi} \frac{x\cos\varphi + y\sin\varphi - R_1}{[(x - R_1\cos\varphi)^2 + (y - R_1\sin\varphi)^2 + d^2]^{3/2}} d\varphi \tag{11}$$

Therefore, the magnetic flux of *Coil2* is

$$\Phi_1 = \frac{\mu_0 R_1 I_1}{4\pi} \oint\int_0^{2\pi} \frac{x\cos\varphi + y\sin\varphi}{\left[(x - R_1\cos\varphi)^2 + (y - R_1\sin\varphi)^2 + d^2\right]^{3/2}} \times d\varphi dS \tag{12}$$

In order to calculate the mutual inductance more conveniently, the plate is considered to be composed of concentric circular coils of different radii. Φ_{ij} is the magnetic flux of the coil with radius R_j from the one with radius R_i. Thus, the total magnetic flux of the plate is

$$\Psi = \sum_1^i \sum_1^j \Phi_{ij} \tag{13}$$

The mutual inductance can be obtained:

$$M = \frac{\Psi}{I_1} \tag{14}$$

Programme according to (1), (2) and from (11) to (14). Figure 3 shows the relationship between length of the copper strip and dM, differential of mutual inductance, near initial position obtained from the programme, which presents good linearity. Through the above analysis, it can be inferred that the initial velocity of the plate is linear with the length of copper strip.

IV. EXPERIMENT & SIMULATION

A. EXPERIMENT AND SIMULATION ABOUT LAUNCHER

1) EXPERIMENT AND ANALYSIS

The experiment platform of EML armor was established as shown in Figure 4. High-voltage power supply is used for charging the pulse capacitors. Current is measured by an external integral standard Rogowski coil. The high-speed camera is used to capture the flight process and calculate the initial velocity of the plate. The experimental circuit

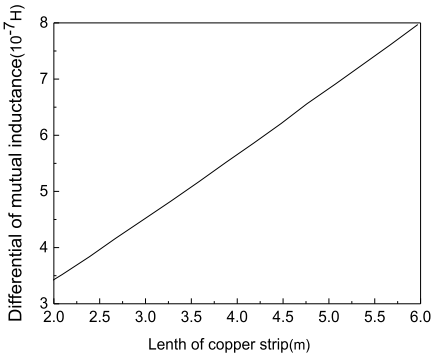

FIGURE 3. The relationship between *dM* and L.

(a) Experimental site

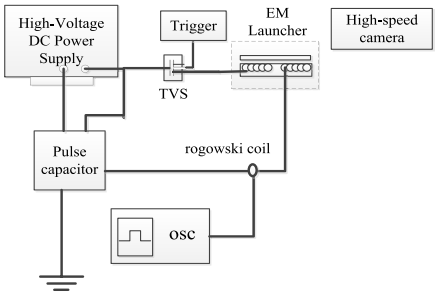

（b） Experimental system schematic

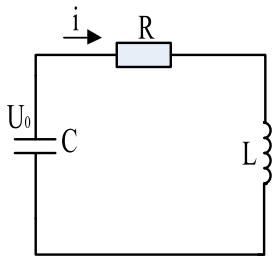

（c） Experimental circuit

FIGURE 4. Experiment system.

is shown in Figure 4(c), where the pulse capacitor, vacuum trigger switch, and launching coil are connected in series to form an RLC circuit. The power source is a 16 μF pulse capacitor with 10kV initial charging voltage. The total resistance is about 30mΩ and the copper coil with 15mm base circle radius, 76mm outer radius is made by a copper strip with a thickness of 2mm, width of 20mm, and length of 5m.

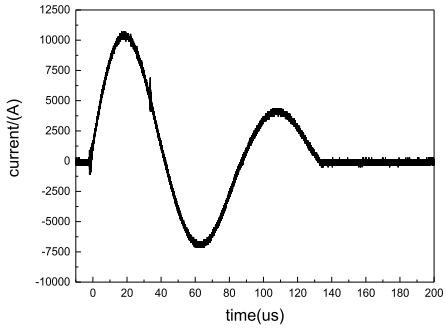

FIGURE 5. Current-time curve of the experiment.

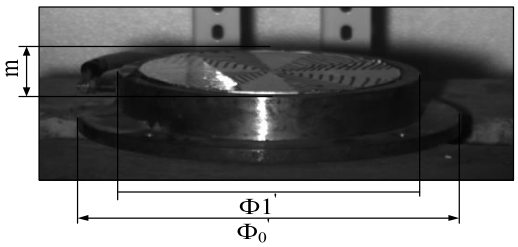

FIGURE 6. Stationary plate and its sizes on the photo.

Figure 5 shows the current-time curve obtained from experiment. The exposure time of the experimental camera is 0.25ms, so from the second frame, all the recorded is projectile movement of the plate. Because the action duration of gravity and air resistance is short, it can be considered that the velocity of projectile movement is the initial velocity. Figure 6 shows the stationary plate and its sizes on the photo.

There is an angle between projection axis and launch direction as shown in Fig. 7(a). In Fig. 7(b), O_1 and O_2 are the actual positions of the center of the plate at two frames respectively, and d stands for the distance between the two on the photo, that is, the projection of O_1O_2. Calculating the angle is necessary for obtaining the initial velocity.

Some measurement can be obtained from Figure 7, including the edge flange diameter and outer diameter of coil-container in the vertical shooting direction and the outer diameter of coil-container along the shooting direction. The scale can be calculated by dividing the diameter of the edge flange taken from the figure by the actual size. And as demonstrated in Fig.7(c), by dividing the outer diameter of coil-container in the vertical direction by the one in the shooting direction, the sine of the angle between the two axes can be obtained. Table 2 displays the measured values mentioned above and calculation results.

Figure 8 displays the position of the plate at frame 25 (left) and frame 40 (right). The center mark of the plate can be clearly recognized, and the distance between the two marks is 36 pixels. The initial velocity of the plate can be obtained by combining the geometric relationship of Fig. 7(b).

$$V_0 = kd/(\Delta t \cos\alpha) \tag{15}$$

So the initial velocity is calculated as 5.7m/s.

TABLE 2. Measured values and caculation results.

edge flange diameter		measured outer diameter of coil-container	
actual size Φ_0/mm	in vertical shooting direction Φ_0'/p	in vertical shooting direction Φ_1'/p	along shooting direction m/p
234	410	320	66
scale		angle between two axes	
0.57		sinα=0.21	

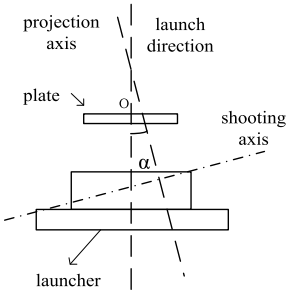

（a） angle between projection and shooting axis

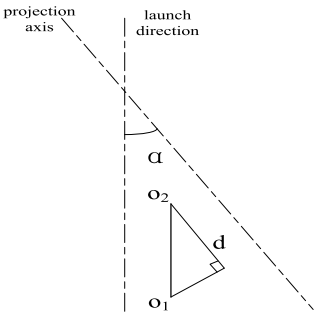

（b） calculation error due to the angle

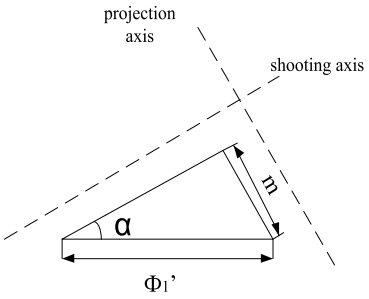

（c） calculation of the angle between the two axes

FIGURE 7. Angle between projection and shooting axis and its calculation.

2) SIMULATION AND ANALYSIS

As shown in Figure 9, the launcher was 3D modeled and imported into Ansys Maxwell 16 for simulation.

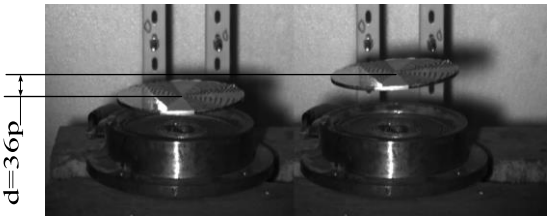

FIGURE 8. Two frames of the plate in projectile state.

The three-dimensional transient field solver is used to apply RLC external circuit excitation without a diode stack. Solution field and motion field are defined as air. The initial velocity and the current are simulated while the pulse capacitor, with initial charge voltage of 10kV, is 16 μf,24 μf, and 32 μf respectively.

It can be seen from Fig. 10 (a) that as the capacitance increases, the peak value and the duration of the current increase. Fig. 10(b) shows that as the capacitance increases, the initial velocity of the plate also increases accordingly. Since the slope of the first rising edge of the current is basically the same, the acceleration in the corresponding acceleration section is basically the same. When the current passes zero, the electromagnetic force between the plate and the coil disappears and the speed remains constant. When the capacitance is 16 μF, the simulation velocity is 7.14 m/s, which is greater than the experimental velocity of 5.7 m/s. This can be explained from the following aspects. a) Although the air domain is defined in the simulation, the air resistance during acceleration cannot be calculated, which will result in a simulation speed higher than the experimental speed. b) In the loading process, there is not only the axial thrust between the coil and the plate, but also the radial force in both, which will cause the deformation of the plate and the coil, thus changing the mutual inductance between the two reduces the thrust and lowers the initial velocity. c) From the perspective of energy, the radial deformation of the coil consumes a part of the electrical energy, so that the kinetic energy obtained by the plate is reduced.4)The phenomenon of breakdown discharge can not be excluded between two adjacent turns of the coil. Although the coil-container make it difficult to be photographed, it can be inferred from spark captured in

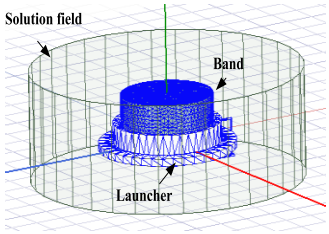

(a) simulation model

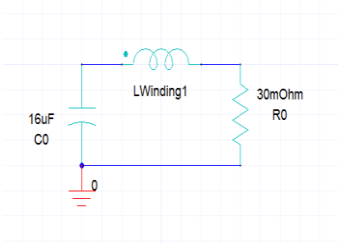

(b) circuit without diode stack

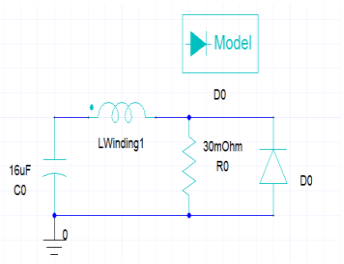

(c) circuit with diode stack

FIGURE 9. Model and external circuit for 3D transient field simulation.

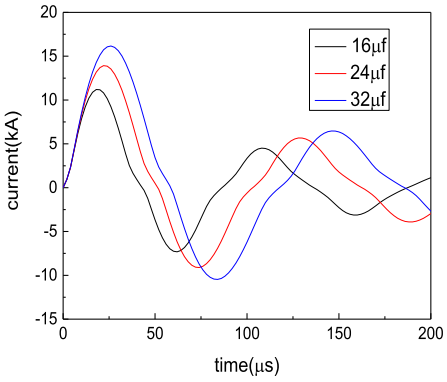

(a) current-time curve under different capacitor

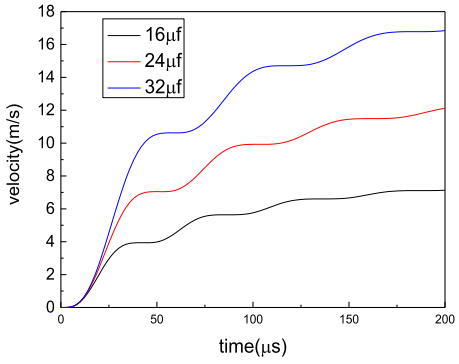

(b) velocity-time curve under different capacitor

FIGURE 10. Current and velocity curve from simulation on prototype launcher.

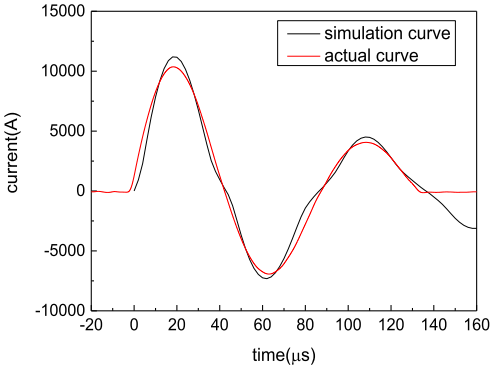

FIGURE 11. Comparison of current-time curve between experiment and simulation.

several experiments, as well as the blackening of some parts of the coil, the plate and coil-container after the launch. So the velocity from simulation is acceptable. Moreover, the linear law between velocity and capacitance is maintained, which satisfies the law described in (9). Figure 11 is a comparison of simulation and experiment results of the current. It can be found that there is a high degree of consistency in both the amplitude characteristics and the time characteristics. The reasons for some differences are the same as those mentioned above, and will not be further elaborated.

In summary, the simulation can not only satisfy the accuracy, but also reflect the objective law. The simulation is used for further study.

B. EFFECT OF COIL GEOMETRIC PARAMETERS ON INITIAL VELOCITY

1) EFFECT OF COPPER STRIP LENGTH ON INITIAL VELOCITY

Modeling and simulation are based on the data listed in Table 1. Nine sets of coils with thickness of 2mm and length between 2m and 5.5m, respectively, are from C1 to C9. Figure 12 is the simulation results of nine sets of coils.

In the current curve family of Fig. 12(a), on the first peak, from top to bottom is C1 to C9. In the family of velocity curves in Figure 12(b), the top-down order is C1 to C9. It can be seen from Fig. 12 that as the length increases, the current oscillation period increases and its peak value decreases, which means the total inductance is increased. Because the rising rate and peak value of C1 current are the highest in the first rising edge, the acceleration of C1 is also highest in the corresponding time-history curve, while those of C9 is the lowest, as it is shown in Fig. 13. However, the current duration of C1 is the shortest, the duration of the thrust of C1 is also the shortest, and the initial velocity of C1 is the lowest while C9 the highest. In this experiment, the driving capability of a 16 μf capacitor with charging voltage of 10 kV is not great, so the acceleration section

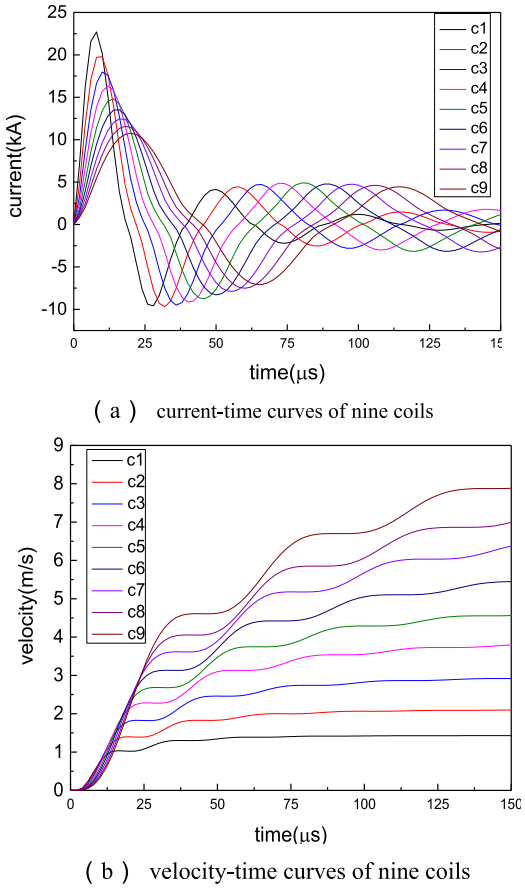

(a) current-time curves of nine coils

(b) velocity-time curves of nine coils

FIGURE 12. Simulation results of coils of different lengths with 2 mm thickness.

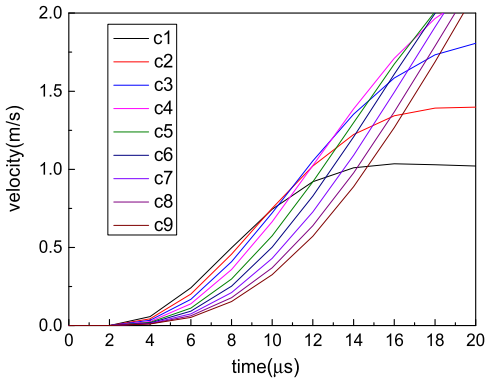

FIGURE 13. Velocity-time curve of each coil in the first 20us.

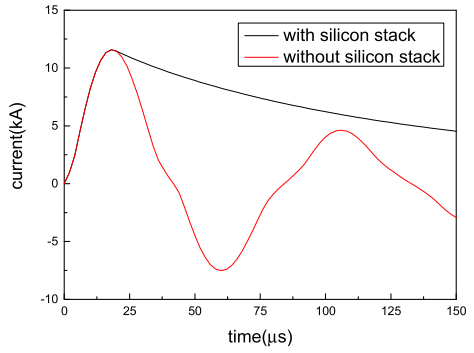

(a) current-time curves of the coil

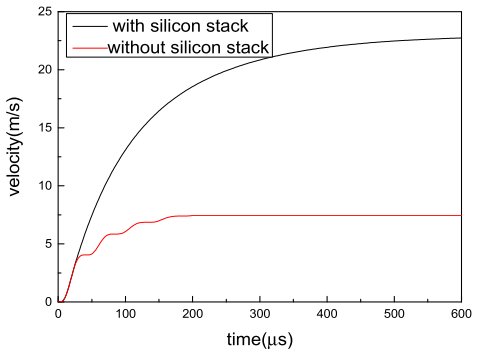

(b) velocity-time curves of the coil

FIGURE 14. Current and velocity curves of the coil with thickness of 2mm and length of 5m.

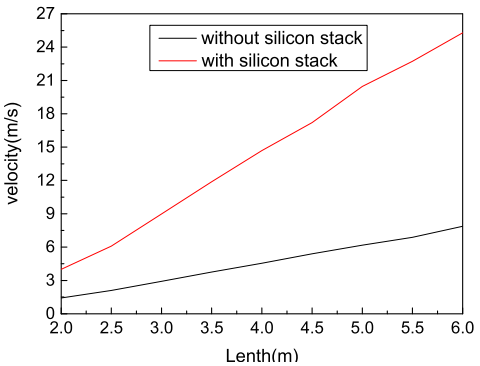

FIGURE 15. Velocity-length relationship of coils with thickness of 2mm at 600μs.

runs through the entire discharge duration, that is, there is no sufficient displacement for the plate to deviate from the coupling region within 150 μs. In this case, the main acceleration process is not completed on the first rising edge. Therefore, the diode stack is added on the original circuit to increase current duration, and the same simulation is performed. The external circuit is shown in Figure 9 (c).

The velocity and current curves of the coil with copper strip length of 5m are shown in Fig.14. After the silicon stack is added, the reverse charging of the capacitor is prevented and the duration of discharging is much longer, which significantly increased thrust duration. Therefore the initial velocity increased greatly and the energy efficiency is improved.

It can be seen from the curves in Fig. 12(b) that after the first rising edge, even if the same moment is taken in different acceleration stages, the relationship between corresponding velocity of nine coils is linear with their length. In fact, it is the same even if the silicon stack is added in the circuit. Figure 15 shows the velocity of each group of coils with and without silicon stack at a specific moment. It can be found that the linear characteristics are obvious.

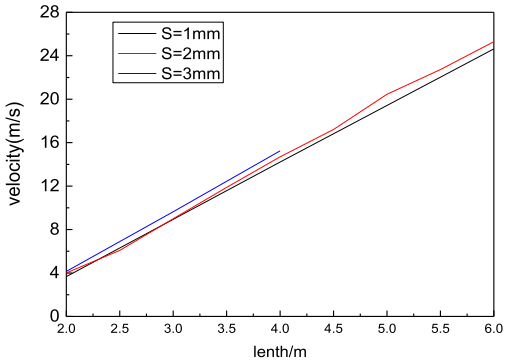

FIGURE 16. Velocity-length relation under different thickness at 600μs.

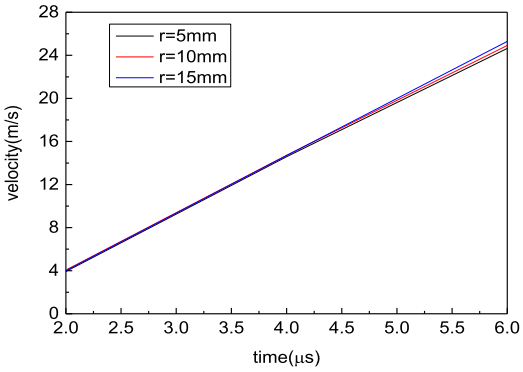

FIGURE 17. Velocity-length relationship under different base circle radius at 600μs.

Through the above analysis, it can be found that the velocity of the flying plate at a certain moment is linear with the length of the coil, regardless of the circuit structure (independent of the presence or absence of the silicon stack). After the silicon stack is added, the current no longer oscillates, the thrust duration is prolonged, and the initial velocity is significantly increased. Therefore, in the subsequent analysis, the circuit with the silicon stack is used for simulation.

2) EFFECT OF COPPER STRIP LENGTH ON INITIAL VELOCITY UNDER DIFFERENT THICKNESS

Coils of different lengths were modeled and simulated with thicknesses of 1 mm, 2 mm, and 3 mm, respectively. Fig. 16 displays velocity-length curves of three different thickness and it can be found that the three are almost parallel and the curves of coils with thickness of 3mm,2mm and 1mm are in order from top to bottom. In the case of the same length, the greater the thickness, the higher the velocity. However, this improvement is small and compromises the ability of the coil-container to accommodate the coil, because the length is shortened. As shown in Fig. 16, when the thickness of copper is 3mm, the longest copper strip can be accommodated is 4 m, and at this time the distance between adjacent copper strips is very close, which is not conducive to the casting of insulating layer. When the cross-section thickness is 1 mm, it can accommodate longer coils, which is beneficial to enhance the launching capacity. However, with the decrease of the cross-section size and the increase of the length of copper strip, the circuit resistance will also increase continuously. In addition, with the continuous reduction of the cross-section size, the anti-radial deformation ability of the coil becomes worse, which is not conducive to the stability of the insulation layer and may damage the insulation layer.

3) EFFECT OF COPPER LENGTH ON INITIAL VELOCITY UNDER DIFFERENT RADIUS OF BASE CIRCLE

Coils of different lengths were modeled and simulated with base circle radius of 5mm, 10mm, and 15mm, respectively. Fig. 17 shows the velocity-length relationship under three different base circle radius. As can be seen from Figure 17, the three straight lines are not parallel, and as the length of the copper strip increases, the three straight lines intersect twice respectively. Simply changing the radius of the base circle does not enhance the launching ability of coils of arbitrary length. Table 3 shows the slope of velocity-length line corresponding to different radius of base circle.

TABLE 3. Slope of velocity-length line corresponding to different radius of base circle.

Base circle radius/r (mm)	Slope/k
5	5.18
10	5.21
15	5.32

As can be seen from Table 3, the slope increases with the increase of base circle radius, but the it is not obvious. The reduction of base circle radius will make the coil-container accommodate longer copper strips to improve the launching ability. However, as radius of base circle radius decreases, the winding of the coil will be more difficult.

V. CONCLUSION

Using the high-speed camera, the self-developed electromagnetic armor launcher is experimented and the initial velocity is calculated. The reliability and accuracy of the simulation are varified by the experimental data. On this basis and combining with the theory, the influence of coil geometric parameters on the velocity is studied by the simulation. Finally, the following conclusions are obtained.

(1)When the outer diameter of the coil is fixed, the initial velocity of the coil increases with the increase of the length of the copper strip, and it shows a good linearity.

(2)With other conditions unchanged, increasing the thickness of the copper strip can increase the initial velocity, but the effect is limited.

(3)Changing the radius of the base circle of the coil has no obvious effect on the initial velocity, but with the increase of the radius of the base circle, the ratio of the initial velocity to the length of the copper strip increases.

Although this paper has obtained some research results, it does not include the influence of the length of the copper strip on the launch performance under the condition that

the outer diameter of the coil is different. In the future, we should focus on the relationship between copper strip length and coil-container size and the initial velocity of the flying plate, and reveal the decisive factors affecting the launch performance.

REFERENCES

[1] H. D. Fair, "Guest editorial the past, present, and future of electromagnetic launch technology and the IEEE international EML symposia," *IEEE Trans. Plasma Sci.*, vol. 41, no. 5, pp. 11–16, May 2013, doi: 10.1109/TPS.2015.2405702.

[2] W. Ma and J. Lu, "Thinking and study of electromagnetic launch technology," *IEEE Trans. Plasma Sci.*, vol. 45, no. 7, pp. 1071–1077, Jul. 2017, doi: 10.1109/TPS.2017.2705979.

[3] P. Lehmann, "Overview of the electric launch activities at the French-German Research Institute of Saint-Louis (ISL)," *IEEE Trans. Magn.*, vol. 39, no. 1, pp. 24–28, Jan. 2003, doi: 10.1109/tmag.2002.805917.

[4] I. R. McNab, "Launch to space with an electromagnetic railgun," *IEEE Trans. Magn.*, vol. 39, no. 1, pp. 295–304, Jan. 2003, doi: 10.1109/TMAG.2002.805923.

[5] K. Sterzelmeier, V. Brommer, and L. Sinniger, "Active armor protection-conception and design of steerable launcher systems fed by modular pulsed-power supply units," *IEEE Trans. Magn.*, vol. 37, no. 1, pp. 238–241, Jan. 2001, doi: 10.1109/20.911829.

[6] T. Zhang, W. Dong, W. Guo, B. Cao, Z. Su, X. Sun, M. Li, and W. Fan, "Spatial movement analysis on the intercepting projectile in the active electromagnetic armor," *IEEE Trans. Plasma Sci.*, vol. 45, no. 7, pp. 1302–1307, Jul. 2017, doi: 10.1109/TPS.2017.2705158.

[7] H.-B. Jin, Y.-J. Cao, Y.-Z. He, and J. Wu, "Optimal design for flat coin electromagnetic launcher," *Ordnance Ind. Autom.*, vol. 28, no. 5, pp. 46–49, May 2009.

[8] Y. Chi, *Research on Induced Current Distribution of Active Electromagnetic Armor*. Harbin, China: Harbin Univ. Science Technology, 2011.

[9] W. Yezhong, H. Zhengxiang, and X. Ming, "The research on motion characteristic of electromagnetic flying plate," *Rockets, Missiles Guid.*, vol. 32, no. 3, pp. 214–216, Jun. 2012.

[10] X. Hui, H. Zhengxiang, and Z. Xudong, "Optimum structural design of electromagnetic launch drive coil," *Chin. Sci. paper*, vol. 8, no. 8, pp. 824–828, Aug. 2013.

[11] Q. Guanyuan, *Circuit*. Beijin, China: Higher Education Press, (in chinese), 2006, pp. 160–161.

ENLING TANG was born in 1971. He received the Ph.D. degree from the Beijing Institute of Technology, Beijing, China, in 2007.

He is currently a Professor and the Ph.D. supervisor of the Nanjing University of Science and Technology, Nanjing, China. His current research interests include electromagnetic launch technology, hypervelocity impact, plasma diagnostic, and impact light flash.

TIANZHI ZHENG was born in Liaoning, China, in 1991. He received the B.S. degree from the School of Mechanical Engineering, Nanjing University of Science and Technology, Nanjing, China, in 2014.

He is currently pursuing the M.S. degree with the School of Equipment Engineering, Shenyang Ligong University.

YAFEI HAN was born in 1979. She received the master's and Ph.D. degrees in signal and information processing from the Information and Communication Engineering College, Harbin Engineering University, Harbin, China, in 2006 and 2011, respectively.

She is currently an Associate Professor. Since 2012, she has been an Associate Professor and collaborated with the Intense Dynamic Loading Research Center, Shenyang Ligong University, Shenyang, China. Her current research interests include electromagnetic launch technology, digital image processing, radar echo signal processing, particularly algorithms for reconstruction of temperature fields of plasma created by hypervelocity impact.

CHUANG CHEN was born in 1987. He received the Ph.D. degree from the Nanjing University of Science and Technology, Nanjing, China, in 2015.

He is currently an Associate Professor. Since 2018, he has been an Associate Professor and collaborated with the Intense Dynamic Loading Research Center, Shenyang Ligong University, Shenyang, China. His current research interests include electromagnetic launch technology, hypervelocity impact, plasma diagnostic, and impact light flash.